# NATIONAL ADVISORY COMMITTEE FOR AERONAUTICS

TECHNICAL NOTE

No. 1236

## DRAG TESTS OF AN NACA $65_{(215)}$-114, a = 1.0 PRACTICAL-CONSTRUCTION AIRFOIL SECTION EQUIPPED WITH A 0.295-AIRFOIL-CHORD SLOTTED FLAP

By John H. Quinn, Jr.

Langley Memorial Aeronautical Laboratory
Langley Field, Va.

Washington

April 1947

NATIONAL ADVISORY COMMITTEE FOR AERONAUTICS

TECHNICAL NOTE NO. 1236

# DRAG TESTS OF AN NACA $65_{(215)}$-114, a = 1.0 PRACTICAL-CONSTRUCTION AIRFOIL SECTION EQUIPPED WITH A 0.295-AIRFOIL-CHORD SLOTTED FLAP

By John H. Quinn, Jr.

## SUMMARY

Drag tests were conducted of an NACA $65_{(215)}$-114, a = 1.0 practical-construction airfoil section. The model was of 85-inch chord and was built by an aircraft manufacturer as representative of the construction method contemplated for the wing of a fighter airplane. The model was equipped with a 0.295-airfoil-chord extensible slotted flap.

The tests consisted of drag measurements over a wide range of Reynolds number and over a small range of section lift coefficient for the model with various surface conditions. The effects of deflecting the flap and sealing the gap on the lower airfoil surface were also investigated.

By improving the surface smoothness and by decreasing the surface waviness, the section drag coefficient at a lift coefficient of 0.1 and at a Reynolds number of $20 \times 10^6$ was decreased from 0.0045 for the original condition to 0.0038, and at a Reynolds number of $40 \times 10^6$, from 0.0053 to 0.0048. The Reynolds number at which the drag began to increase with Reynolds number was shifted from $12 \times 10^6$ to $20 \times 10^6$. For the model with a standard production finish, the drag coefficient increased with Reynolds number from a value of 0.0039 at a Reynolds number of $18 \times 10^6$ to a value of 0.0055 at a Reynolds number of $62 \times 10^6$. Between Reynolds numbers of $62 \times 10^6$ and $80 \times 10^6$ the section drag coefficient for this condition was essentially constant. Waxing the model surfaces produced no change in the drag characteristics of the airfoil at least at Reynolds numbers between $16 \times 10^6$ and $36 \times 10^6$.

Deflecting the flap $4^\circ$ increased the section drag coefficient for the model with the production finish from 0.0039 to 0.0046 at a lift coefficient of 0.1 and at a Reynolds number of $16 \times 10^6$. The center of the low-drag range of lift coefficient was increased from a lift coefficient of 0.08 to 0.18. Sealing the gap on the lower

surface reduced the minimum drag coefficient with flap deflected from 0.0046 to 0.0044, and reduced the range of lift coefficient for low drag from 0.3 to 0.2. The center of the low-drag range, however, was increased thereby from 0.18 to 0.22.

## INTRODUCTION

Drag tests were made in the Langley two-dimensional low-turbulence pressure tunnel of an NACA $65_{(215)}$-114, a = 1.0 practical-construction airfoil section. This airfoil section was equipped with a 0.295-airfoil-chord slotted flap and is representative of the root section of a fighter airplane.

The variation of drag with Reynolds number was measured at approximately the design section lift coefficient for various surface conditions and flap configurations. Drag measurements were made at several Reynolds numbers over a small range of section lift coefficient and over a part of the model span at one lift coefficient. The surface waviness was also determined for various surface conditions. In addition to evaluating the merits of the construction method as affecting the extent of laminar flow that could be obtained, tests were made to determine the aerodynamic effects of a standard production finishing process and the effects on drag of the cruising deflection of the slotted flap both with and without a seal over the gap.

## SYMBOLS

| | |
|---|---|
| c | airfoil chord |
| $c_d$ | section drag coefficient |
| $c_l$ | section lift coefficient |
| s | distance from airfoil leading edge measured along surface |
| x | distance along airfoil chord from leading edge |
| d | difference between reading of curvature gage when mounted on flat surface and at point on airfoil surface |
| d/c | waviness index |
| R | Reynolds number based on airfoil chord |

$\delta_f$ flap deflection

$\delta$ effective boundary-layer thickness, distance from airfoil surface to point inside boundary layer where inside velocity is equal to 0.707 of velocity outside boundary layer

$R_\delta$ Reynolds number based on effective boundary-layer thickness

$U$ local velocity outside boundary layer

$U_o$ free-stream velocity

## DESCRIPTION OF MODEL

The model was built to the ordinates of the NACA $65_{(215)}$-114 airfoil section. The ordinates for this section may be obtained by the method outlined in reference 1. The model had a chord of 85 inches and a span of 35.75 inches. The spars center lines were located at 8.2, 37.3, and 68.8 percent chord. Between the front and rear spars the skin was approximately 0.75 inch thick and was built up in the following manner:

| Material | Thickness (in.) |
|---|---|
| Dural inner plate | 0.072 |
| Dural inner skin | .025 |
| Balsa core | .600 |
| Dural outer plate | .040 |
| Dural outer skin | .016 |
| | 0.753 |

The inner plate was cycle-welded to the spars and ribs. The remaining components were sandwiched together and bonded by cycle-weld and, in turn, this sandwich was cycle-welded to the inner plate. Ahead of the front spar the skin thickness tapered down to fair into the nose skin, which was approximately 0.28 inch thick, and was built up of a 0.250 balsa core sandwiched between two dural sheets 0.016 inch thick. Ribs extended from the front to the rear spar at each end of

the model. These ribs were also built up of a balsa-dural sandwich. Spanwise seams in the skin existed on both surfaces at 0.199c and at both the upstream and downstream ends of the middle spar cap. The seams in the neighborhood of the spar were approximately 1/16 inch wide and 1/32 inch deep. The spar cap extended approximately 0.015c upstream and downstream of the middle spar. A pronounced wave existed at the seam located at 0.199c on both surfaces. The spanwise extent of the most pronounced waviness is indicated in figure 1. Spanwise rows of flush rivets were located at approximately 0.095, 0.105, 0.45 and 0.49 chord. A double row of flush rivets extended along both ends of the model between the front and rear spars. Photographs of the model in the bare-metal condition as received from the manufacturer are presented as figure 2. The model was equipped with an extensible slotted flap which had a chord equal to 0.295 airfoil chord. For the airplane cruising condition, the flap nose moves rearward approximately 0.045 airfoil chord and the flap is deflected $4^{\circ}$. In so doing, a gap is formed on the lower surface between the airfoil lip and the flap nose. Figure 3 shows the flap in the retracted and deflected conditions and indicates the position of the simulated door.

## TESTS

The tests were made in the Langley two-dimensional low-turbulence pressure tunnel (designated TDT). The tunnel test section is 3 feet wide and $7\frac{1}{2}$ feet high and was designed to test models spanning completely the 3-foot jet in two-dimensional flow. The turbulence level of this tunnel is only a few hundredths of 1 percent, or considerably below that at which an effect is noticeable on the critical Reynolds number of a sphere. In this tunnel, drag measurements are made by the wake-survey method and lifts are measured by integrating the pressures along the floor and ceiling of the tunnel test section. A large range of Reynolds number was obtained by varying the tunnel tank pressures from 14.7 to 135 pounds per square inch absolute. In no case did the tunnel Mach number exceed 0.2. More complete descriptions of the methods used in obtaining and reducing the data in this tunnel are contained in reference 1.

Waviness measurements were made using an Ames dial gage mounted on legs spaced $2\frac{15}{32}$ inches apart (0.029c) to serve as a waviness indicator. A photograph of the waviness indicator is presented as figure 4. The waviness index d/c was obtained by subtracting the

reading of the indicator when placed on a flat surface from the reading at any point on the airfoil surface and dividing the difference by the airfoil chord.

The model was tested with the following surface conditions:

(a) As received: Bare-metal surfaces.

(b) Production finished: This finish conforms to the specifications in the appendix. The seams at the spar cap on both surfaces were partly filled with glazing putty during the finishing process. A large amount of "orange peel" finish existed in this condition, and there were some checks and inclusions in the paint. Photographs of the model with the production finish are presented in figure 5.

(c) Production finished, wax removed: The model was washed twice with benzol and once with warm soapy water to remove the wax.

(d) Faired at seam: The wave located at the seam at 0.199c on both surfaces was eliminated as nearly as possible by filling the depression with glazing putty and sanding with rubber blocks in a chordwise direction until the putty was featheredged flush with the model surfaces. Several applications of putty were required to eliminate the wave.

(e) Both surfaces glazed and sanded to 0.5c: The orange-peel finish, checks, and inclusions in the paint existing for the production finish were all sanded smooth. All local scratches, nicks, and seams were filled flush with the surface with glazing putty and sanded smooth. Photographs of the model in this condition are presented as figure 6. The extent of the putty which was applied in the fairing process in step (d) may be seen in these photographs. All the light areas shown in these photographs represent improvements in the surface smoothness.

The range of Reynolds number and section lift coefficient over which data were obtained for the various surface conditions are presented in the following table. Measurements of spanwise drag variation and for the flap-deflected configurations are also indicated:

| Surface condition | Reynolds numbers | Lift coefficients | Spanwise measurements | $\delta_f$ (deg) | Gap condition |
|---|---|---|---|---|---|
| (a) | $6 \times 10^6$ to $50 \times 10^6$ | -0.5 to 0.6 | 6 in. right and left on model, center line | 0 | - - - |
| (b) | $8 \times 10^6$ to $80 \times 10^6$ | -.5 to .6 | - - - - - | 0 | - - - |
| (b) | $10 \times 10^6$ to $19 \times 10^6$ | -.4 to .8 | - - - - - | 4 | Open |
| (b) | $10 \times 10^6$ and $18 \times 10^6$ | -.4 to .8 | - - - - - | 4 | Sealed |
| (c) | $16 \times 10^6$ to $36 \times 10^6$ | .08 | - - - - - | 0 | - - - |
| (d) | $10 \times 10^6$ to $40 \times 10^6$ | .08 | - - - - - | 0 | - - - |
| (e) | $10 \times 10^6$ to $40 \times 10^6$ | .08 | - - - - - | 0 | - - - |

## RESULTS AND DISCUSSION

### Waviness Characteristics

Waviness measurements for the NACA $65_{(215)}$-114 practical-construction airfoil section are presented in figures 7 and 8 for different model surface conditions. The locations of various surface irregularities are indicated in figure 7(a) to aid in determining the cause of undue waviness. The seams located at 0.199c and the spar at 0.37c appeared to be the only causes of surface waves on this model. The peak in the variation of waviness index along the surface at a distance s from the leading edge of approximately 0.51c is not a wave, but is caused by the change in curvature found at the point where the airfoil thickness starts decreasing in the direction of flow. The waviness indicated at 0.199c on the upper surface in figure 7(b) and on the lower surface in figures 7(e) and 7(f) is representative of the parts of the airfoil where waves existed at this station. The spanwise extent of these waves was indicated in figure 1. These waves caused a rather large fluctuation in the chordwise variation of the waviness index and appeared to be larger on the lower surface than on the upper surface. The production

finish appeared to produce little change in the waviness characteristics of the wing. A large amount of waviness existed at the spar at 0.37c on both surfaces. It is not likely that this waviness would have a serious effect upon transition because transition only occurs at or behind the minimum pressure point, 0.08c behind the waves, at the lower Reynolds numbers where the flow is least sensitive to disturbances. Calculations have indicated that at a Reynolds number of approximately $30 \times 10^6$ the natural transition point begins to move forward of the minimum pressure point.

The wave at 0.199c, however, which was greater in magnitude and shorter in length than the waviness at the spar, was considered more likely to affect transition. For that reason an attempt was made to remove the wave at that point by filling with putty and sanding. The waviness measurements after the fairing process are shown in figure 8. Practically no waviness existed after the fairing process because a fair curve may be drawn through the measured values that does not deviate from the experimental curve by a value of the waviness index of more than 0.00001 or 0.00002.

## Drag Characteristics

Variation of section drag coefficient with Reynolds number.- The variation of section drag coefficient with Reynolds number is presented in figure 9 at a section lift coefficient of approximately 0.1 for several surface conditions and flap configurations. In the "as-received" condition a minimum drag coefficient of 0.0041 was obtained at a Reynolds number of $12 \times 10^6$, at which Reynolds number the drag coefficient began to increase with increasing Reynolds number and attained a value of 0.0055 at a Reynolds number of $48 \times 10^6$. The production finish decreased the minimum drag coefficient to 0.0039 and increased to $20 \times 10^6$ the Reynolds number at which the drag coefficient began rising. At a Reynolds number of $62 \times 10^6$ the drag coefficient was 0.0055 and remained essentially constant at Reynolds numbers between $62 \times 10^6$ and $80 \times 10^6$. It has been shown that no noticeable decrease in the surface waviness was obtained with the production finish. The surfaces were actually less smooth with the production finish than with the original bare-metal surfaces; but the seams at the spar caps were filled in the process of painting the wing. Filling the seams would not be expected to bring about the reduction in drag shown in figure 9 between the as-received condition and the production finish but would more likely be expected to eliminate a sharp rise in the variation of drag coefficient with Reynolds number. The explanation of the reduction in drag caused by

the production finishing procedure is not evident at present.

The wax on the model was removed and the drag coefficients were measured at several Reynolds numbers between $16 \times 10^6$ and $36 \times 10^6$. The removal of the wax was found to bring about no measurable change in drag coefficient over the Reynolds number range investigated.

The effect of fairing the wave located at 0.199c on the variation of drag coefficient with Reynolds number is also shown in figure 9. A minimum drag coefficient of 0.0038 was obtained for this condition, and the drag coefficient began increasing at a Reynolds number of $20 \times 10^6$ attaining a value of 0.0049 at a Reynolds number of $40 \times 10^6$. Between Reynolds numbers of $20 \times 10^6$ and $40 \times 10^6$ (the highest Reynolds number obtained for this condition) the elimination of the wave produced a reduction in drag coefficient of approximately 0.0002 or 0.0003 below the values for the production finish. Extensive glazing and sanding to produce a very smooth surface brought about little further change in drag, although a tendency toward slightly lower drag coefficients than those for the forward condition was observed at Reynolds numbers between $32 \times 10^6$ and $40 \times 10^6$.

Drag coefficients were calculated for this airfoil at several Reynolds numbers between $30 \times 10^6$ and $80 \times 10^6$; the results of these calculations are presented in figure 9. These calculations were made by assuming that transition occurred at a constant value of $R_\delta = 8000$; the use of this value of $R_\delta$ has been previously found to provide rather good agreement between calculated and experimental drag coefficients. The position of transition at any Reynolds number was then estimated by solving graphically for $x$ in the following expression obtained from reference 2:

$$\frac{R_\delta^2}{R} = (2.3)^2 \left(\frac{U_o}{U}\right)_x^{7.17} \int_0^x \left(\frac{U}{U_o}\right)^{8.17} d\frac{s}{c}$$

After the location of the transition point was estimated, the drag coefficient was calculated by the method presented in reference 3. Drag coefficients were not calculated for Reynolds numbers at which transition would be estimated to occur behind the minimum pressure point.

Figure 9 shows that the variation of drag coefficient with Reynolds

number calculated on the basis that transition occurs at $R_\delta = 8000$ agrees rather well with the experimental results for the glazed and sanded conditions, at least at Reynolds numbers between $30 \times 10^6$ and $40 \times 10^6$. In addition, the calculated variation appears to represent a reasonable extrapolation of the results obtained for the faired and for the glazed and sanded conditions, and, at Reynolds numbers between approximately $64 \times 10^6$ and $80 \times 10^6$, the calculated values are practically the same as experimental values obtained for the model with the production finish.

The variation of drag coefficient with Reynolds number is also presented in figure 9 calculated on the assumption that transition occurred at a constant value of $R_\delta$ of 8500. The differences in the variation of drag coefficient with Reynolds number for the two sets of calculations shown in figure 9 demonstrate the effect of choice of $R_\delta$ upon the correlation obtained with experimental results. An increase in $R_\delta$ increases the Reynolds number at which transition occurs at the minimum pressure point but appears to have little effect on the position of transition, and consequently on the drag coefficient, once transition has moved well forward toward the leading edge of the airfoil. At Reynolds numbers between $64 \times 10^6$ and $80 \times 10^6$ the position of transition as estimated by use of the two values of $R_\delta$ differed not more than 0.01 chord.

Data are also presented in figure 9 for the model with the production finish with the slotted flap deflected $4^\circ$ with the gap on the lower surface both open and sealed. At a lift coefficient of 0.09, deflecting the flap caused a drag increment that varied from 0.0006 at a Reynolds number of $10 \times 10^6$ to 0.0009 at a Reynolds number of $18 \times 10^6$. Sealing the gap appeared to have no effect on the drag at least at a lift coefficient of 0.09 and between Reynolds numbers of $10 \times 10^6$ and $18 \times 10^6$.

Spanwise drag variations.- Spanwise drag surveys at a section lift coefficient of 0.12 are presented in figure 10 for the model in the as-received condition at three Reynolds numbers. The spanwise variations shown are not considered excessive and are representative of the model with other surface conditions.

Effect of Reynolds number on the variation of section drag coefficient with section lift coefficient.- The variations of section drag coefficient with section lift coefficient are presented in figure 11 for various Reynolds numbers, surface conditions, and flap

configurations. Figure 11(a) for the model in the as-received condition and figure 11(b) for the model with the production finish demonstrate the usual effects of Reynolds number. As the Reynolds number increases the range of lift coefficient for low drag decreases, the minimum drag coefficient decreases at first and then increases, and the drag coefficients outside the low-drag range steadily decrease. The data presented in figures 11(c) and 11(d) for the model with the production finish and with the flap deflected 4° are for the gap-open and gap-sealed conditions, respectively. Increasing the Reynolds number from $10 \times 10^6$ to $18 \times 10^6$ brought about a rather small decrease in the low-drag range for the gap-open condition but decreased the low-drag range of lift coefficients from approximately 0.35 to 0.2 for the gap-sealed condition.

Effects of surface condition and flap configuration on the variation of section drag coefficient with section lift coefficient.- For purposes of comparison, the variations of section drag coefficient with section lift coefficient are presented in figure 12 for an approximately constant Reynolds number and for some of the surface conditions and flap configurations tested. The data presented in figure 12 show that at a Reynolds number of $16.0 \times 10^6$ the production finish produced a decrease in section drag coefficient of approximately 0.0003 at lift coefficients between 0 and 0.6 and caused a slight increase in the low-drag range. With the production finish, deflecting the flap 4° increased the low-drag range, increased the minimum drag coefficient from 0.0039 to 0.0046, and shifted the center of the low-drag range of lift coefficients from approximately 0.08 to 0.18. Sealing the gap and increasing the Reynolds number from $16.0 \times 10^6$ to $17.9 \times 10^6$ decreased the low-drag range of lift coefficients from approximately 0.3 to 0.2, decreased the minimum drag coefficient from 0.0046 to 0.0044, and shifted the center of the low-drag range to approximately a lift coefficient of 0.22.

## CONCLUSIONS

Drag tests of the NACA $65_{(215)}$-114, a = 1.0 practical-construction airfoil section led to the following conclusions:

1. In the "as-received" condition, at a lift coefficient of approximately 0.1 the model had a minimum drag coefficient of 0.0041 at a Reynolds number of $12 \times 10^6$, at which point the drag coefficient began increasing with Reynolds number and attained a value of 0.0055 at a Reynolds number of $48 \times 10^6$.

2. Finishing the model in accordance with a production finishing procedure reduced the minimum drag coefficient to 0.0039 between Reynolds numbers of $12 \times 10^6$ and $20 \times 10^6$, at which point the drag coefficient began increasing with Reynolds number and attained a value of 0.0055 at a Reynolds number of $62 \times 10^6$. Between Reynolds numbers of $62 \times 10^6$ and $80 \times 10^6$ the section drag coefficient had an essentially constant value of 0.0055.

3. Fairing a rather sharp wave located at approximately 0.199 airfoil chord on both surfaces reduced the minimum drag coefficient to 0.0038 between Reynolds numbers of $10 \times 10^6$ and $20 \times 10^6$, at which point the section drag coefficient began increasing with Reynolds number and reached a value of 0.0049 at a Reynolds number of $40 \times 10^6$. The model with the production finish without the wave faired had a section drag coefficient of 0.0052 at a Reynolds number of $40 \times 10^6$.

4. Waxing the model surfaces had no effect on the section drag characteristics of the airfoil at least at Reynolds numbers between $16 \times 10^6$ and $36 \times 10^6$.

5. A calculated variation of drag coefficient with Reynolds number appeared to check rather closely with the experimental variation for the model in the best test condition. For the calculation the transition point was assumed to occur at a constant value of Reynolds number based on effective boundary-layer thickness $R_\delta$ of 8000 when this value was reached at or ahead of the minimum pressure point.

6. With the production finish, a $4^\circ$ deflection of the slotted flap increased the minimum section drag coefficient from 0.0039 to 0.0046 at a Reynolds number of $16 \times 10^6$. The center of the low-drag range of section lift coefficients was increased from 0.08 to 0.18 by deflecting the flap.

7. Sealing the gap on the lower surface, which was caused by deflecting the flap, had no effect on the section drag coefficient at a lift coefficient of 0.1, but reduced the low-drag range of section lift coefficients from 0.3 to 0.2. The section drag coefficient at a section lift coefficient of 0.22, however, was 0.0044 for the gap-sealed condition, or 0.0003 less than that for the gap-open condition at the same section lift coefficient.

Langley Memorial Aeronautical Laboratory
National Advisory Committee for Aeronautics
Langley Field, Va., November 6, 1946.

## APPENDIX

The finishing specifications for the NACA $65_{(215)}$-114, a = 1.0 practical-construction section were as follows:

1. Thoroughly clean all exterior metal surfaces with AN-TT-T-256 thinner.

2. Immediately wipe off with clean white dry cloth and thoroughly clean the metal surfaces.

3. Apply a uniform wet film of aircraft-type liquid rust remover to the clean surfaces with a brush or clean white rag soaked in the solution. Allow the surface-treating solution to remain in contact for 3 to 5 minutes. Maintain a continuous wet film during this period of time. Dilute one part to two parts of water by volume and use at room temperature. Entirely remove the residue by wiping with a clean white dry cloth.

4. Apply by spray operation a semitransparent coat of zinc-chromate primer conforming to specification AN-TT-P-656 used with the following reduction: two and one-half parts of toluol substitute (spec. AN-T-8b) to one part primer. Allow a drying time of $\frac{1}{2}$ to 1 hour.

5. Use glazing putty in excessively deep depressions. Apply with putty knife, or squeeze in one or more coats to allow for shrinkage, until the putty is completely flush with the surface. Smooth either with a solvent saturated rag or sandpaper to eliminate any roughness.

6. Apply two coats of quick-drying synthetic primer to all seams, rivets, joints, nicks, and scratches on the airplane. Allow sufficient drying time between coats before sanding with No. 280 or No. 320 wet or dry sandpaper. Apply a third coat of quick-drying synthetic primer over the entire surface, adding one part of sea-blue lacquer to obtain a colored undercoat. Sand final coat with No. 320 sandpaper. Dilute the quick-drying synthetic primer three parts to one part thinner.

7. Apply two cross coats of high-gloss sea-blue lacquer ($80^{\circ}$ to $90^{\circ}$ gloss). Reduce two parts lacquer to three parts thinner. (Three coats of lacquer were applied. The thinner was diluted three parts thinner to one part retarder.)

8. Sand final coat of lacquer with No. 600 sandpaper.

9. Allow to dry overnight.

10. Rub surfaces with automotive-type lacquer rubbing compound.

11. Rub surfaces with finishing compound.

12. Polish surfaces with combination liquid wax and rubbing compound.

## REFERENCES

1. Abbott, Ira H., von Doenhoff, Albert E., and Stivers, Louis S., Jr. Summary of Airfoil Data. NACA ACR L5C05, 1945.

2. Jacobs, E. N., and von Doenhoff, A. E.: Formulas for Use in Boundary-Layer Calculations on Low-Drag Wings. NACA ACR, Aug. 1941.

3. Tetervin, Neal: A Method for the Rapid Estimation of Turbulent Boundary-Layer Thicknesses for Calculating Profile Drag. NACA ACR No. L4G14, 1944.

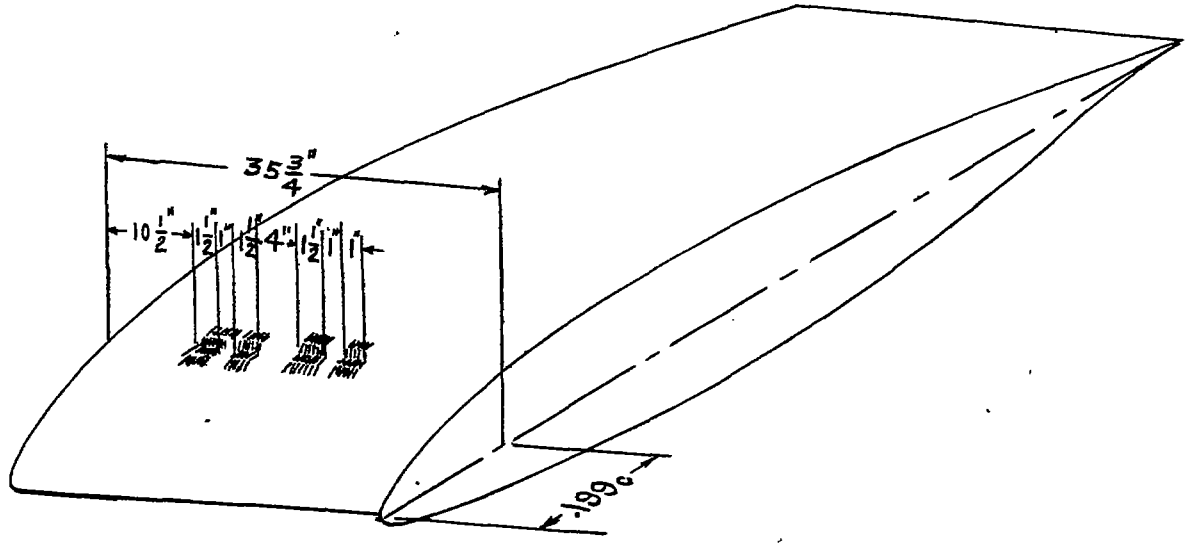


(a) Upper surface.

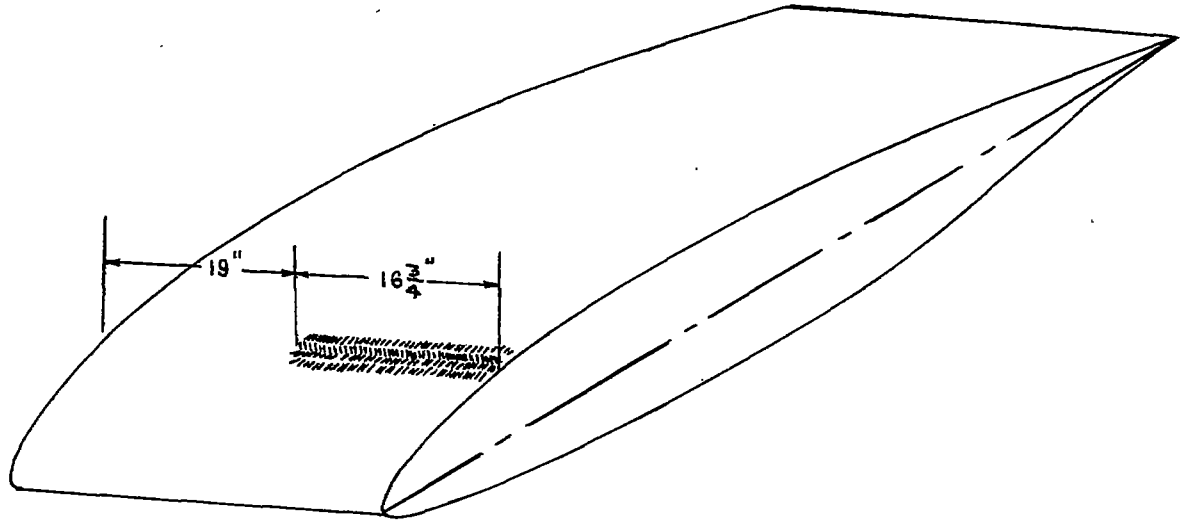


(b) Lower surface.

NATIONAL ADVISORY COMMITTEE FOR AERONAUTICS

Figure 1.- Spanwise extent of surface waves located at 0.199c on both surfaces of NACA 65(215)-114, a = 1.0 practical-construction airfoil section.

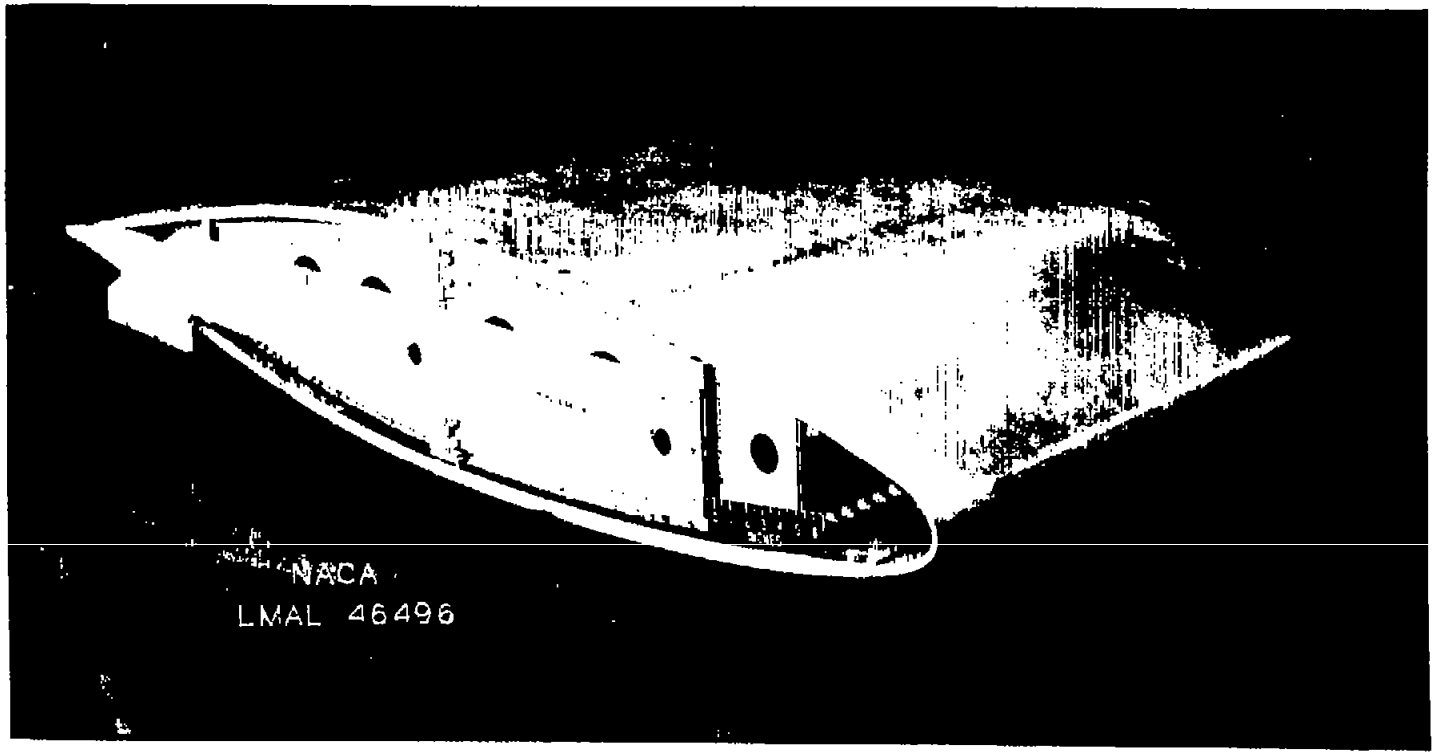


(a) Upper surface.

Figure 2.- NACA $65_{(215)}$-114 practical-construction airfoil section.

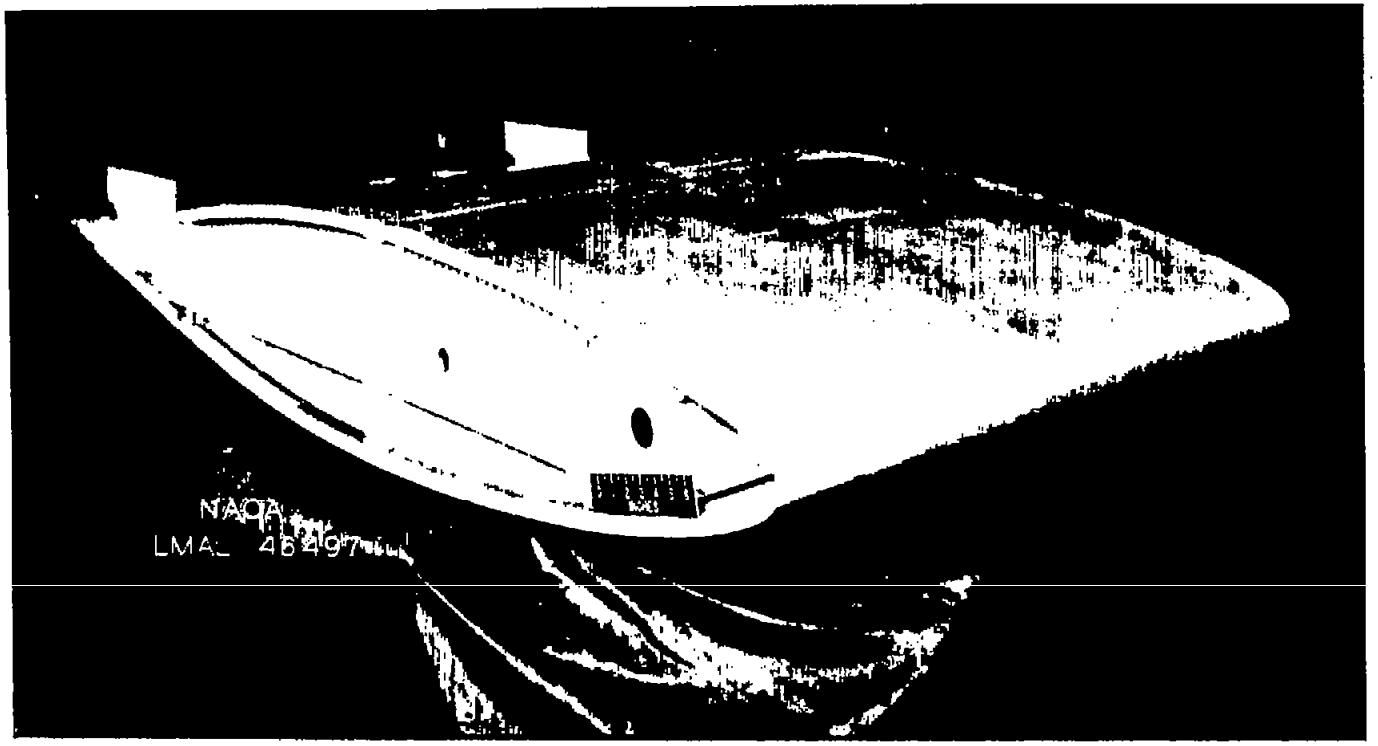


(b) Lower surface.

Figure 2.- Continued.

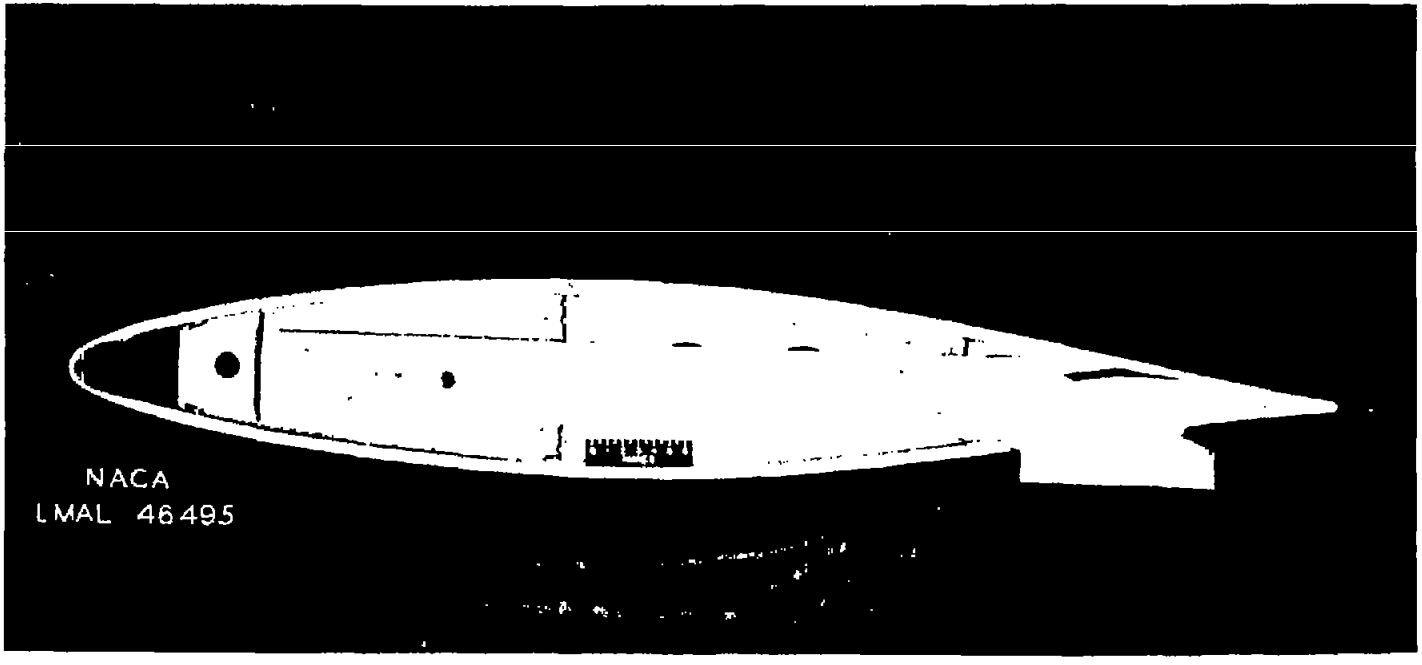


(c) End view.

Figure 2.- Concluded.

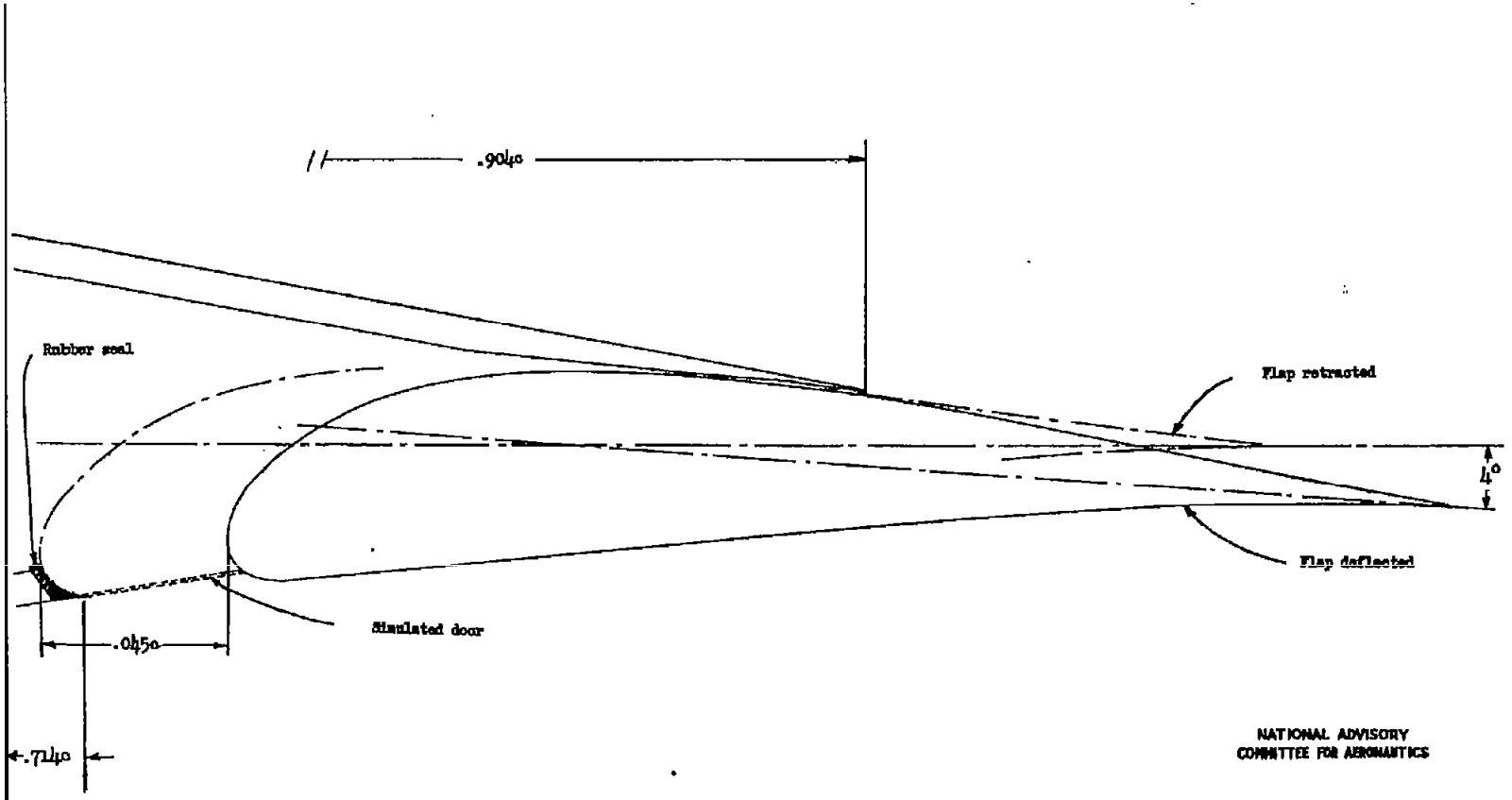


Figure 3.- Flap for NACA 65(215)-114 practical-construction airfoil section in retracted and deflected position.

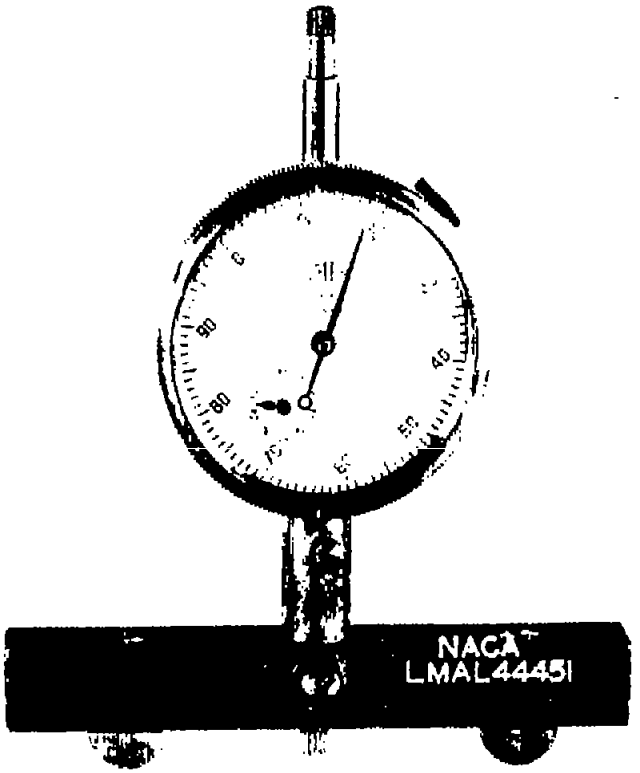


Figure 4.- Ames dial gage mounted on legs to serve as a waviness indicator.

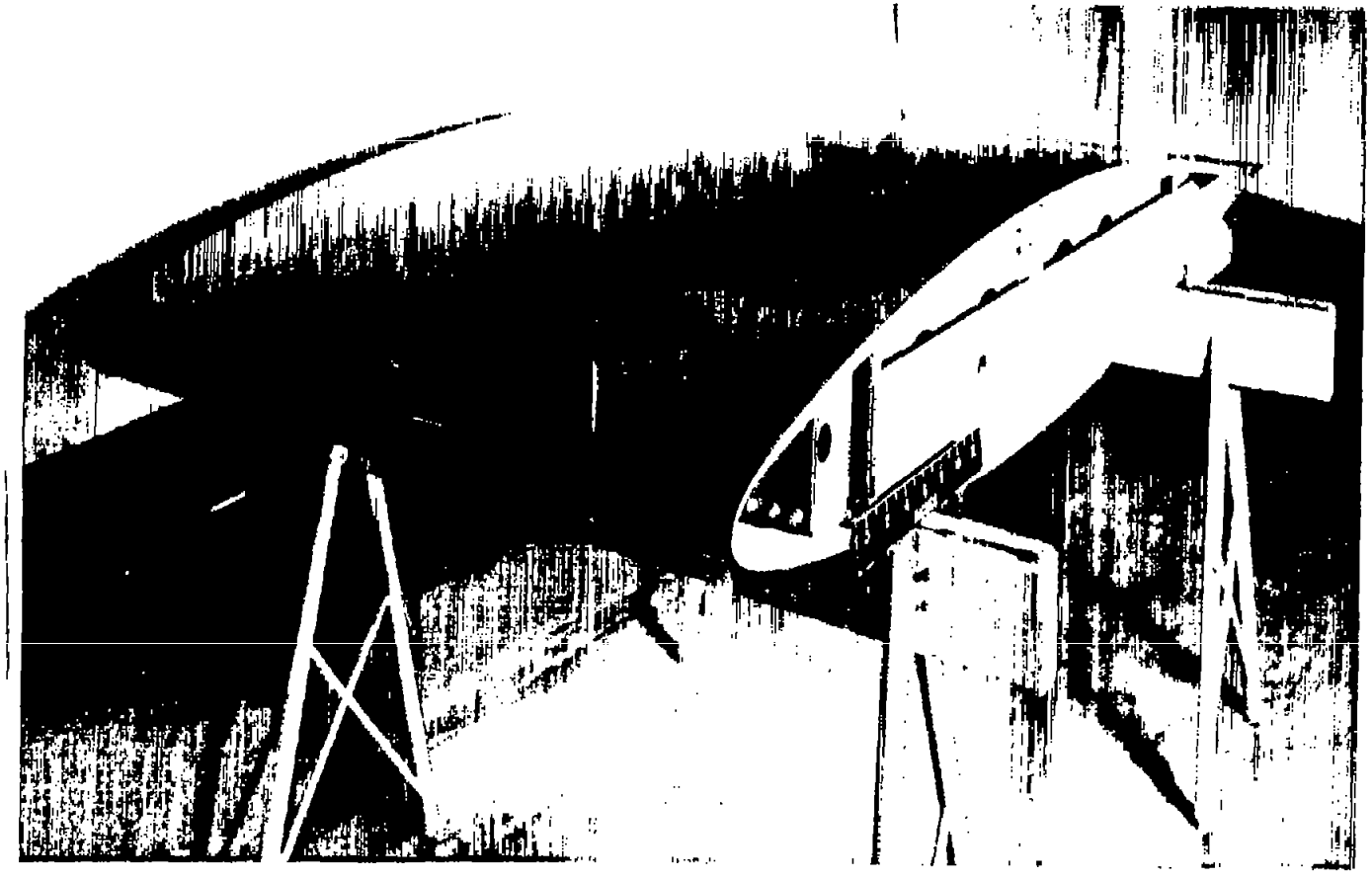

(a) Upper surface.

Figure 5.- NACA $65_{(215)}$-114 practical-construction airfoil section with production finish.

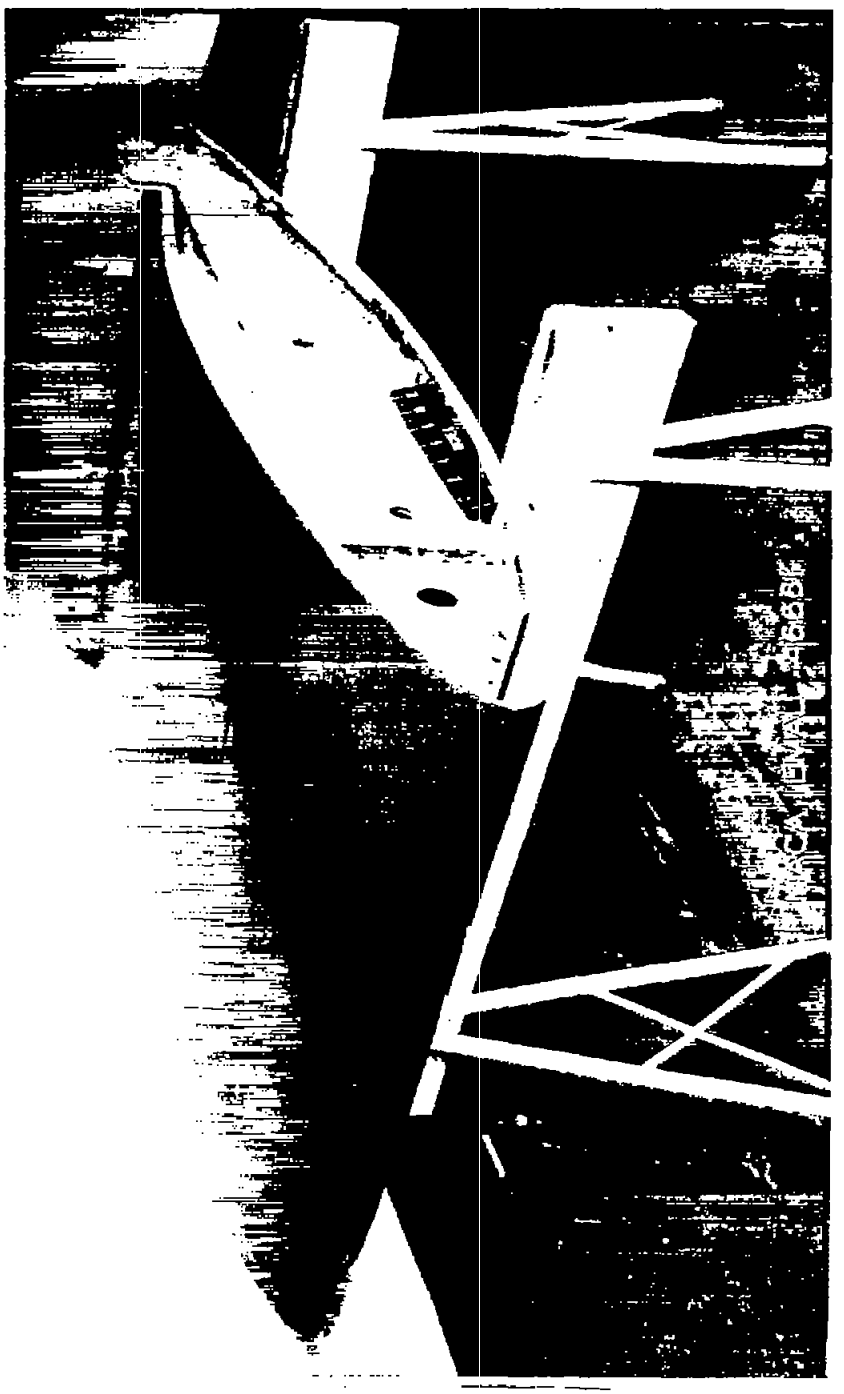

(b) Lower surface.

Figure 5.- Concluded.

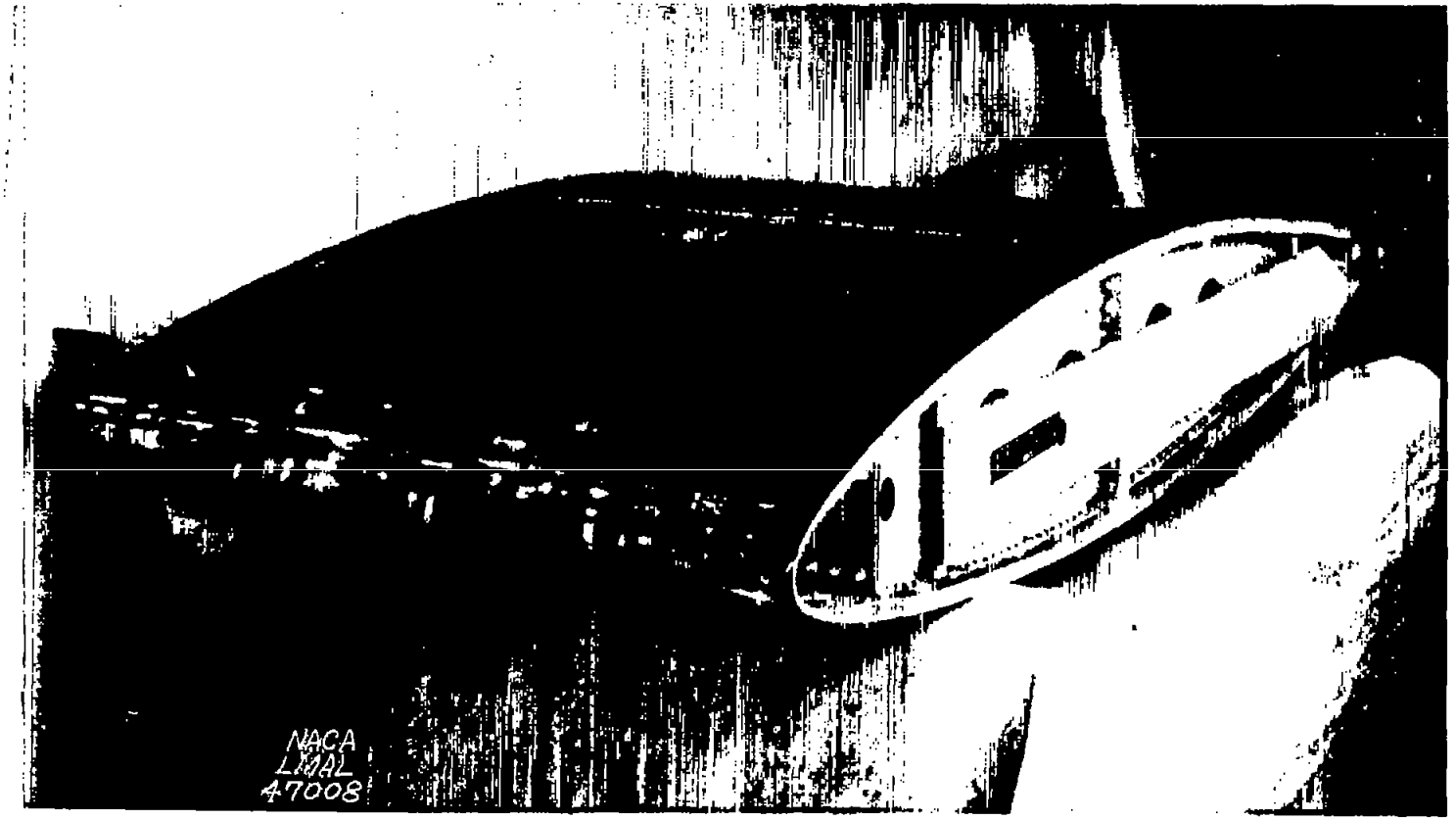


(a) Upper surface.

Figure 6.- NACA $65_{(215)}$-114 practical-construction airfoil section with model surfaces glazed and sanded to 0.5c.

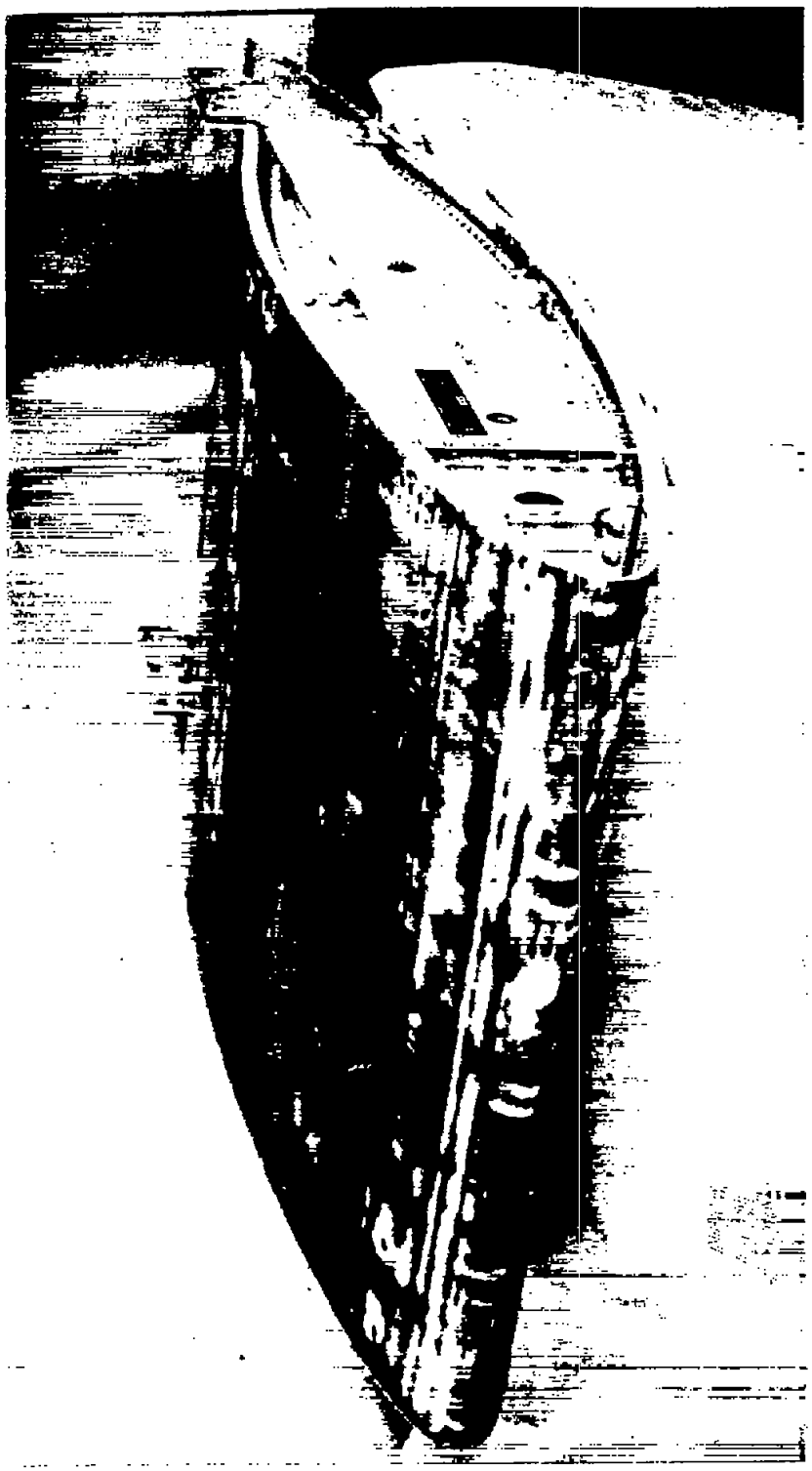

(b) Lower surface.

Figure 6.- Concluded.

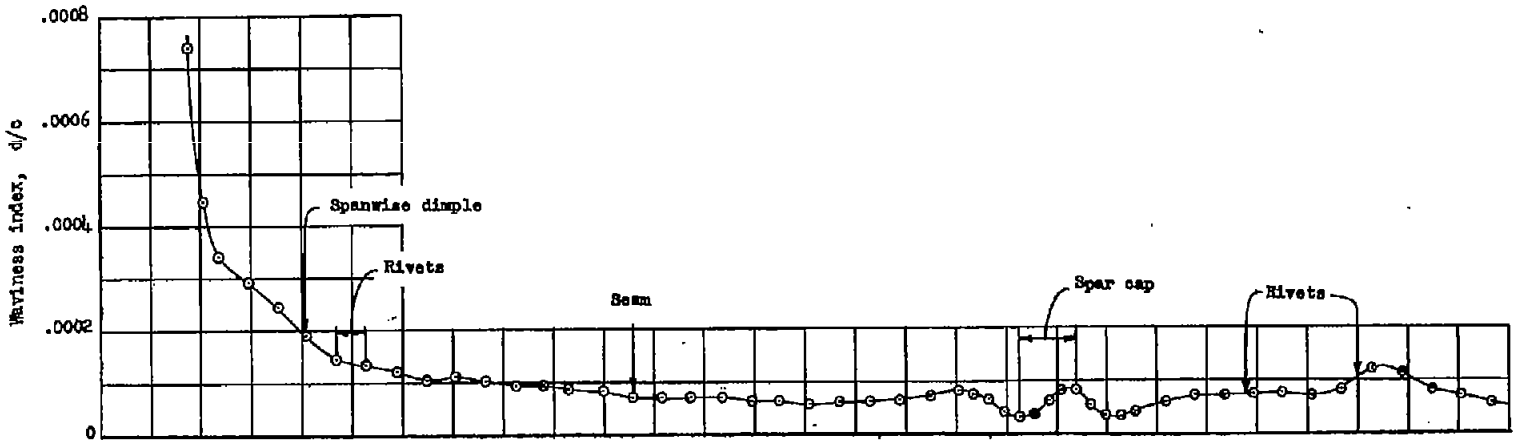


(a) Upper surface center line; as received.

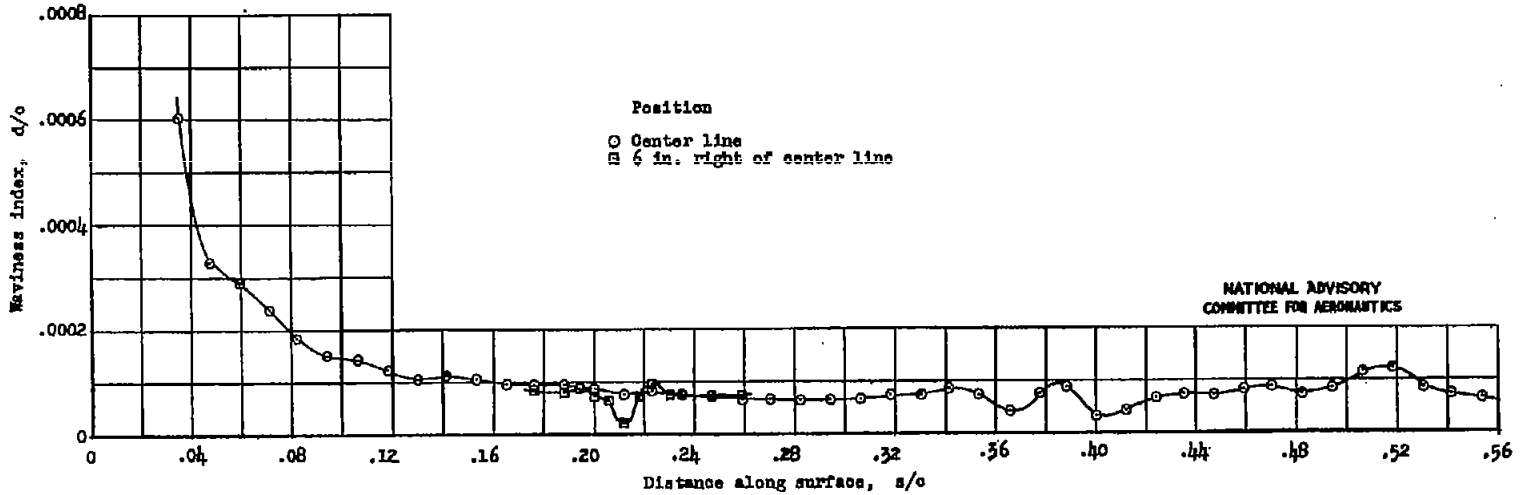


(b) Upper surface center line and 6 inches right of model center line; production finish.

Figure 7.- Waviness measurements on NACA 65(215)-114 practical-construction airfoil section in "as-received" condition and with production finish.

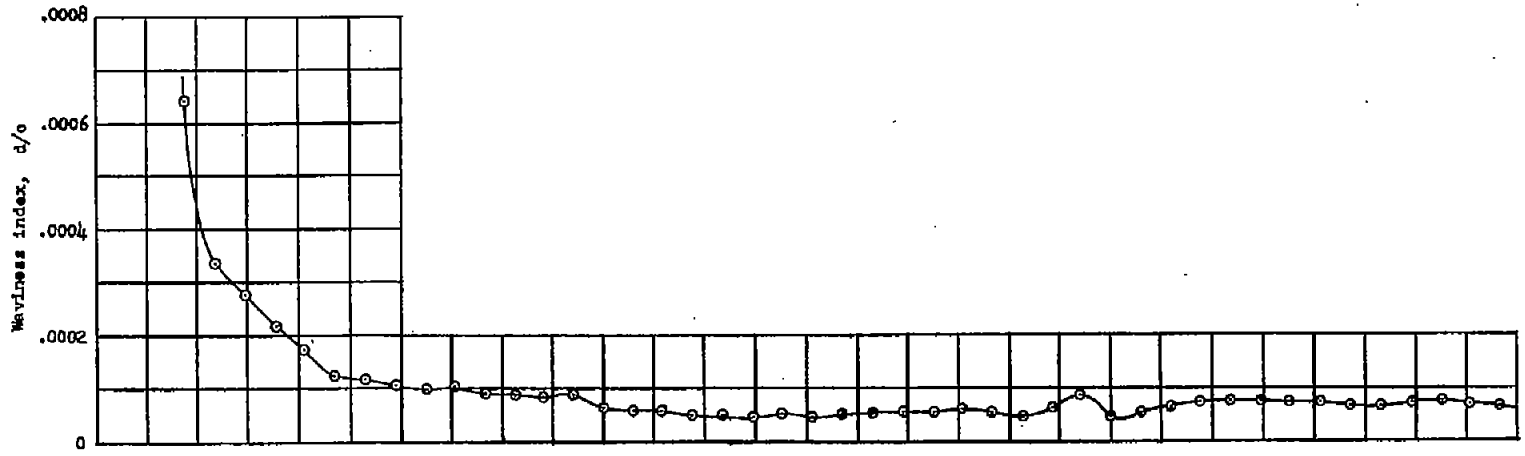


(c) Lower surface center line; as received.

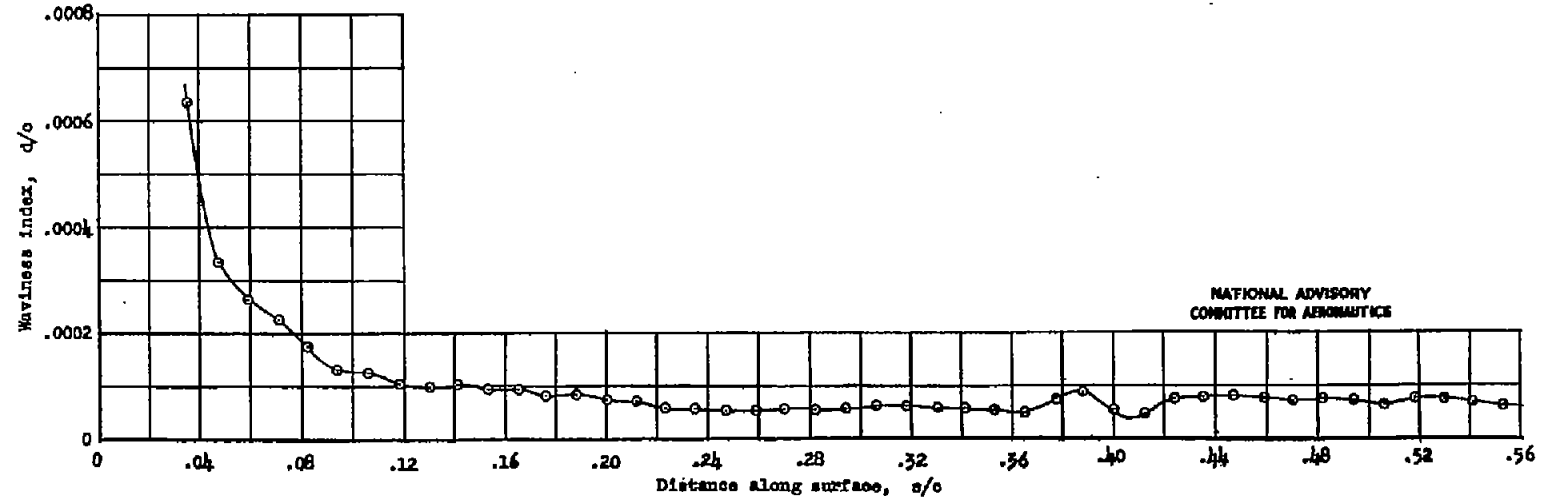


(d) Lower surface center line; production finish.

Figure 7.- Continued.

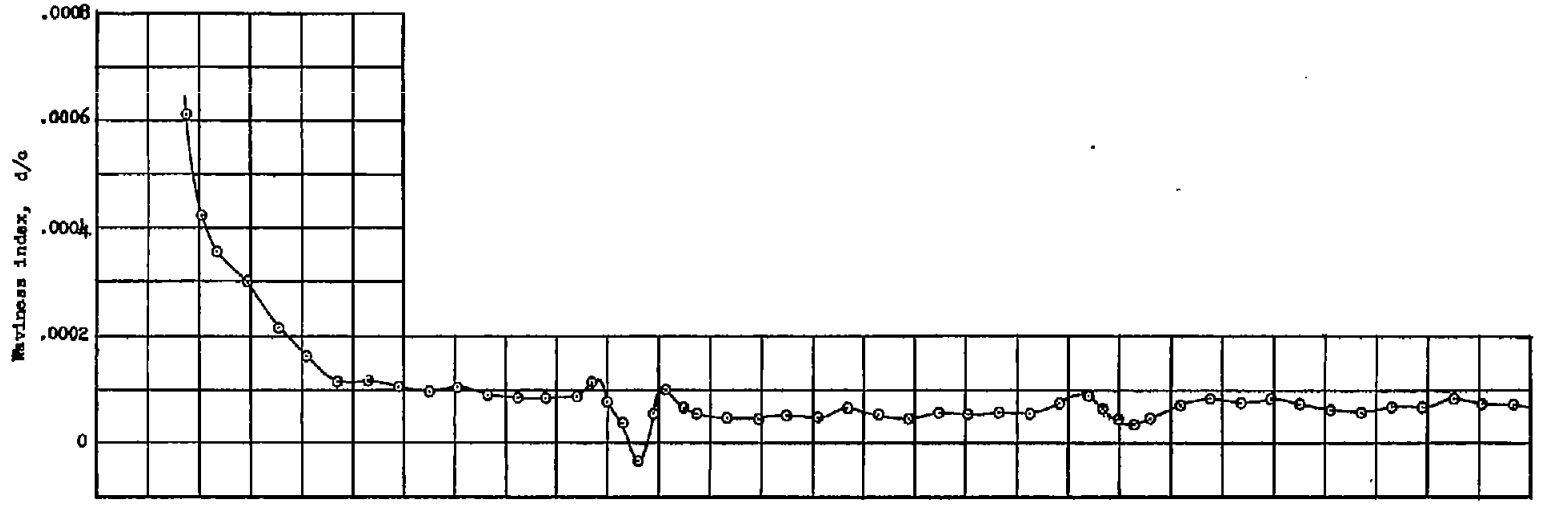


(e) Lower surface, 3 inches right of model center line; as received.

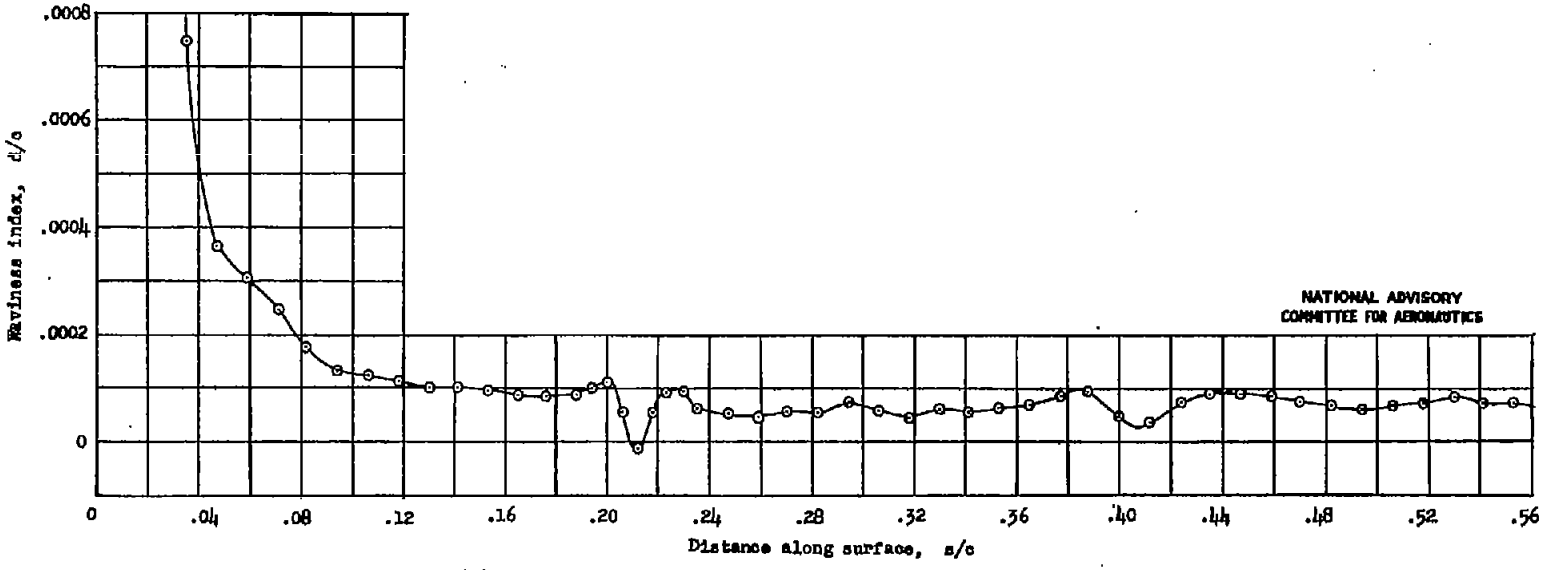


(f) Lower surface, 3 inches right of model center line; production finish.

Figure 7.- Concluded.

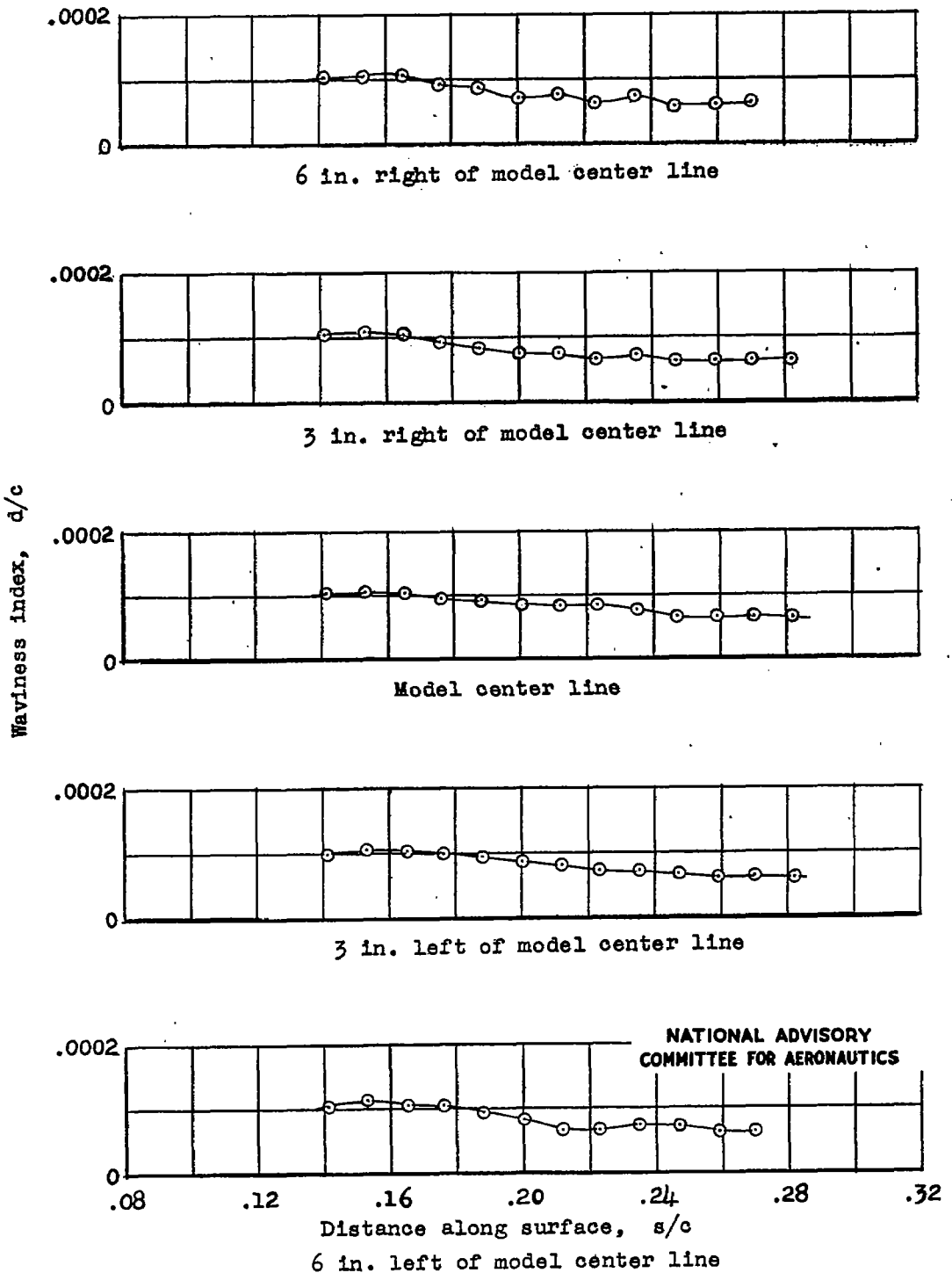


(a) Upper surface.

Figure 8.- Waviness measurements of NACA 65(215)-114 practical-construction airfoil section with wave faired at 0.199c.

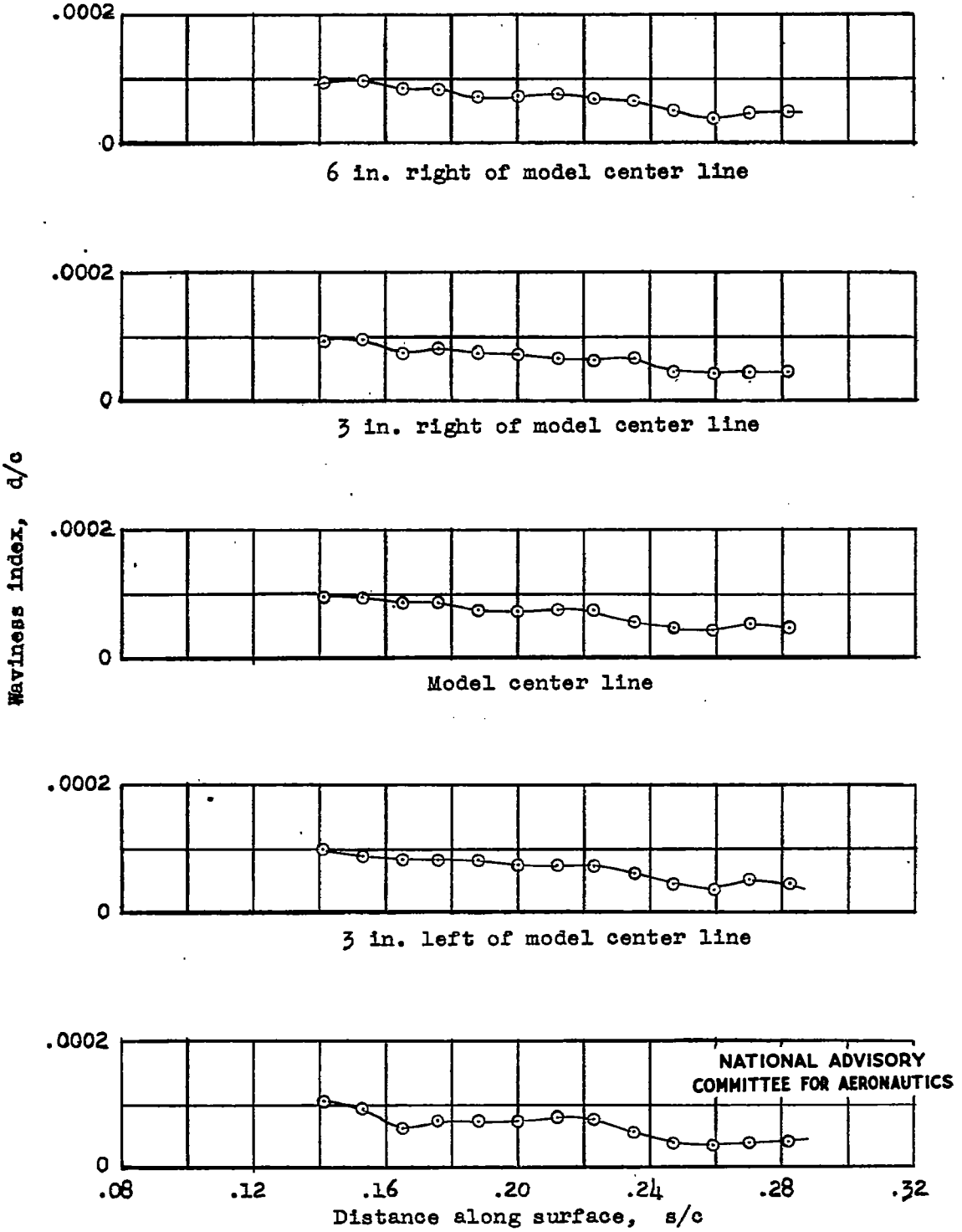


(b) Lower surface.

Figure 8.- Concluded.

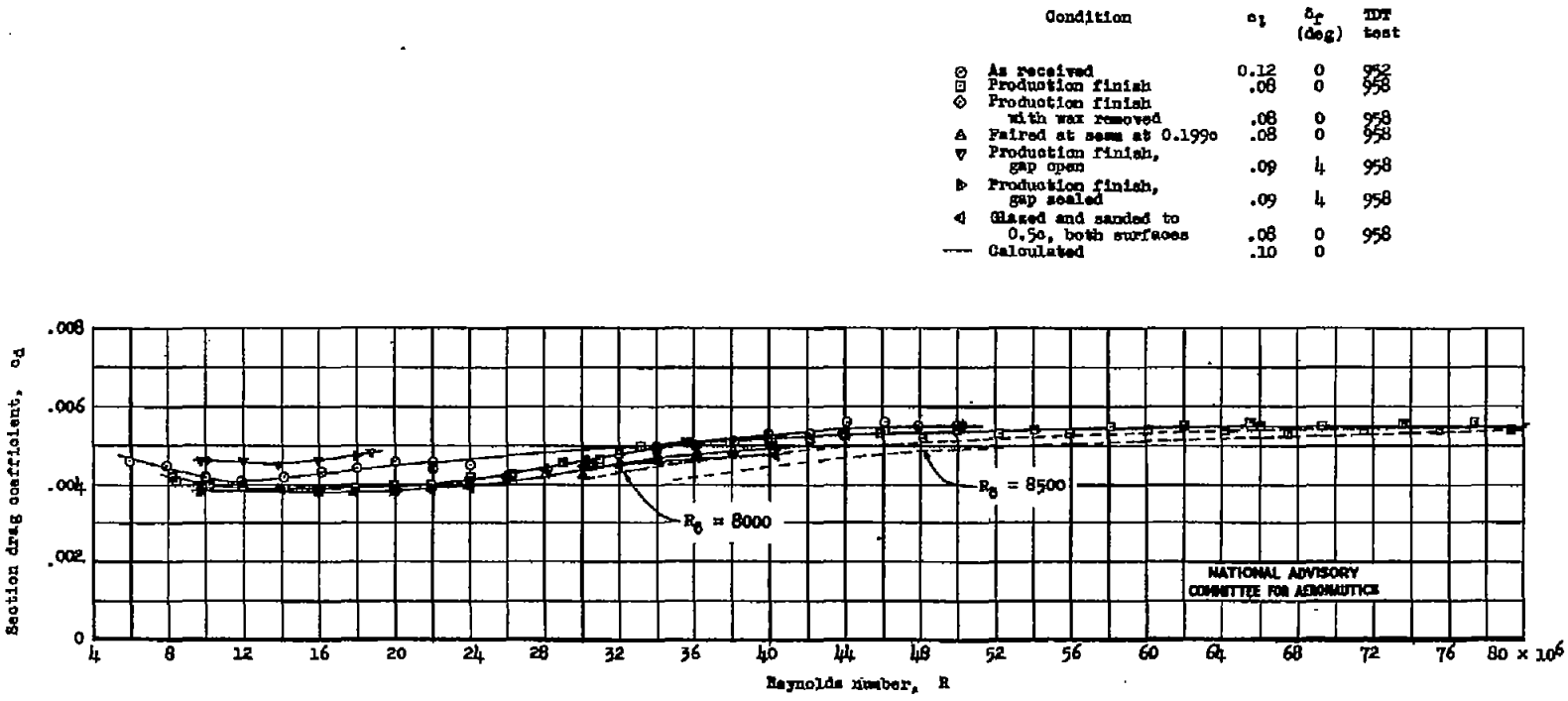


Figure 9.- Variation of section drag coefficient with Reynolds number for NACA 65(215)-114 practical-construction airfoil section with various surface conditions and flap deflections.

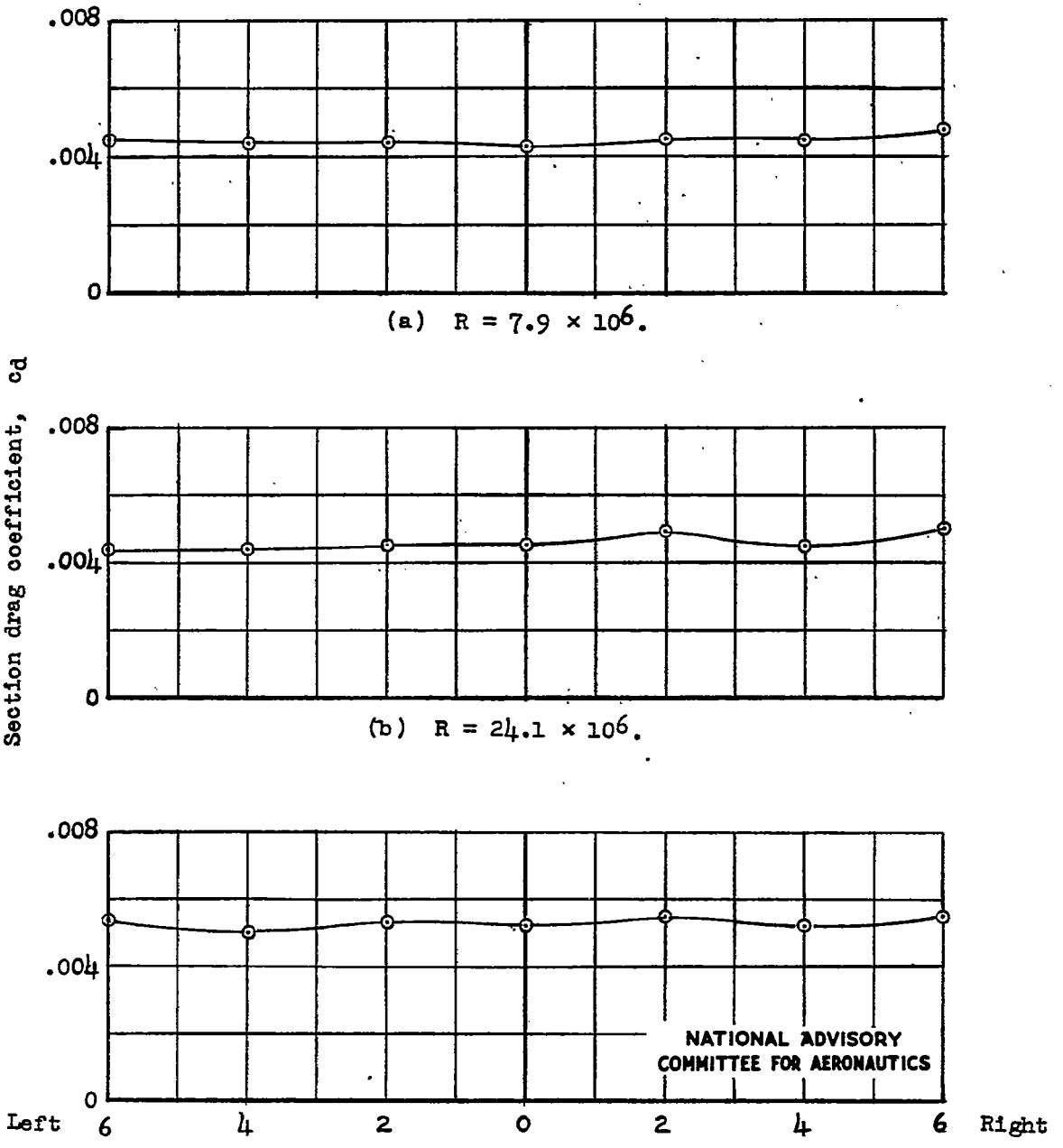


Figure 10.- Spanwise drag variation of NACA 65(215)-114 practical-construction airfoil section in as-received condition. $c_l$ = 0.12; test, TDT 952.

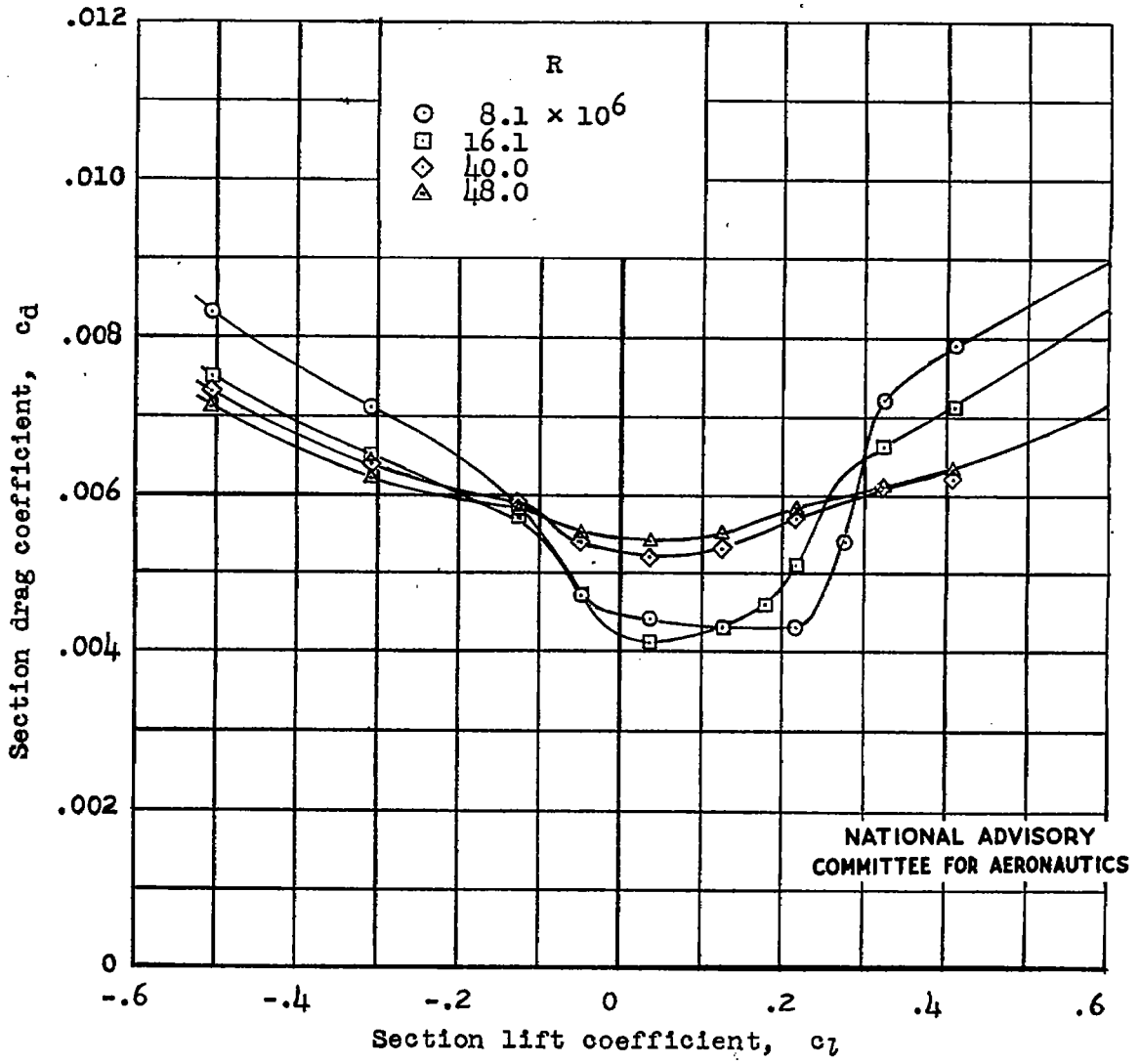


(a) Model as received; flap retracted; test, TDT 952.

Figure 11.- Variation of section drag coefficient with section lift coefficient for NACA 65(215)-114 practical-construction airfoil section for various surface conditions and flap deflections.

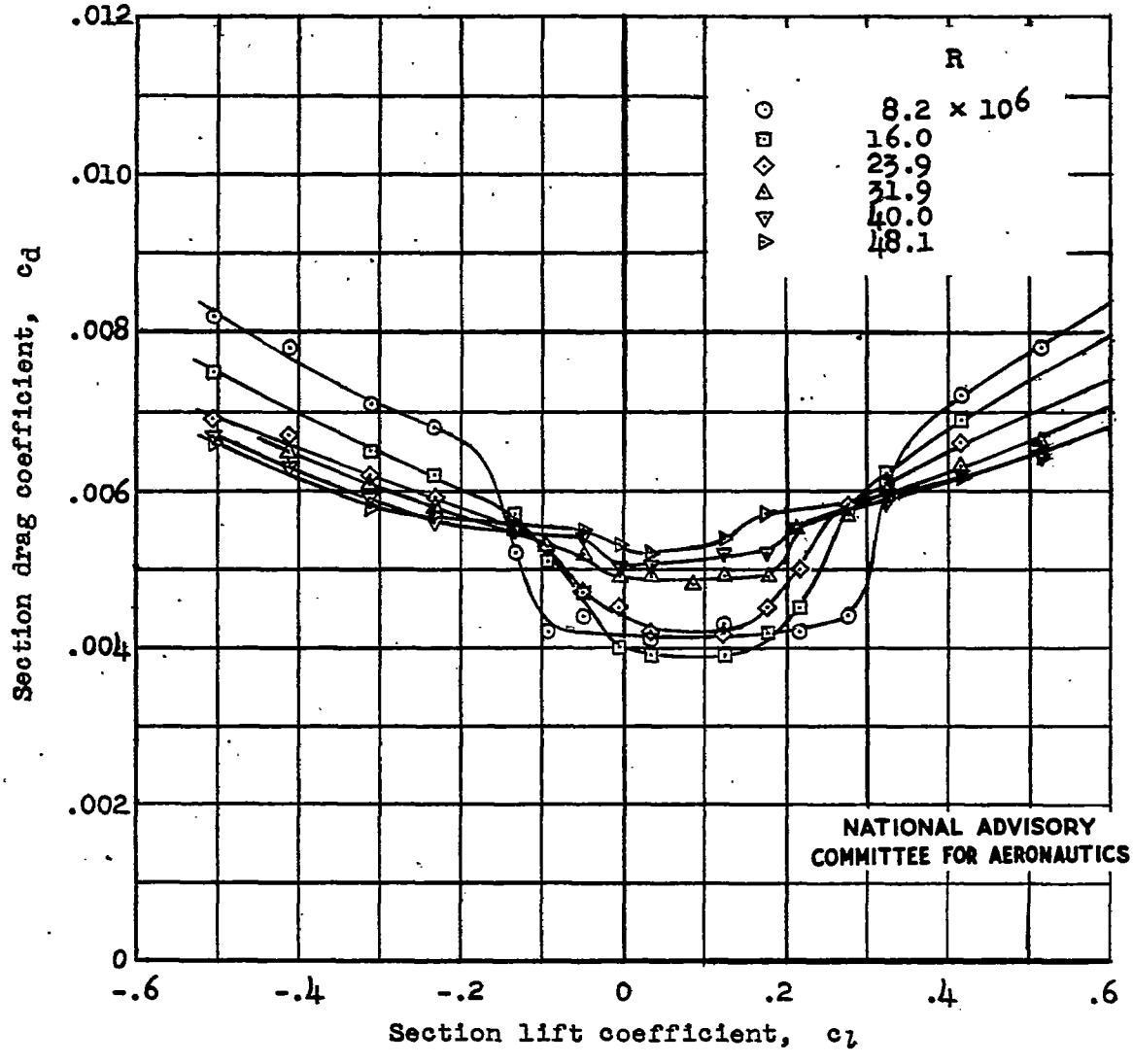


(b) Model with production finish; flap retracted; test, TDT 958.

Figure 11.- Continued.

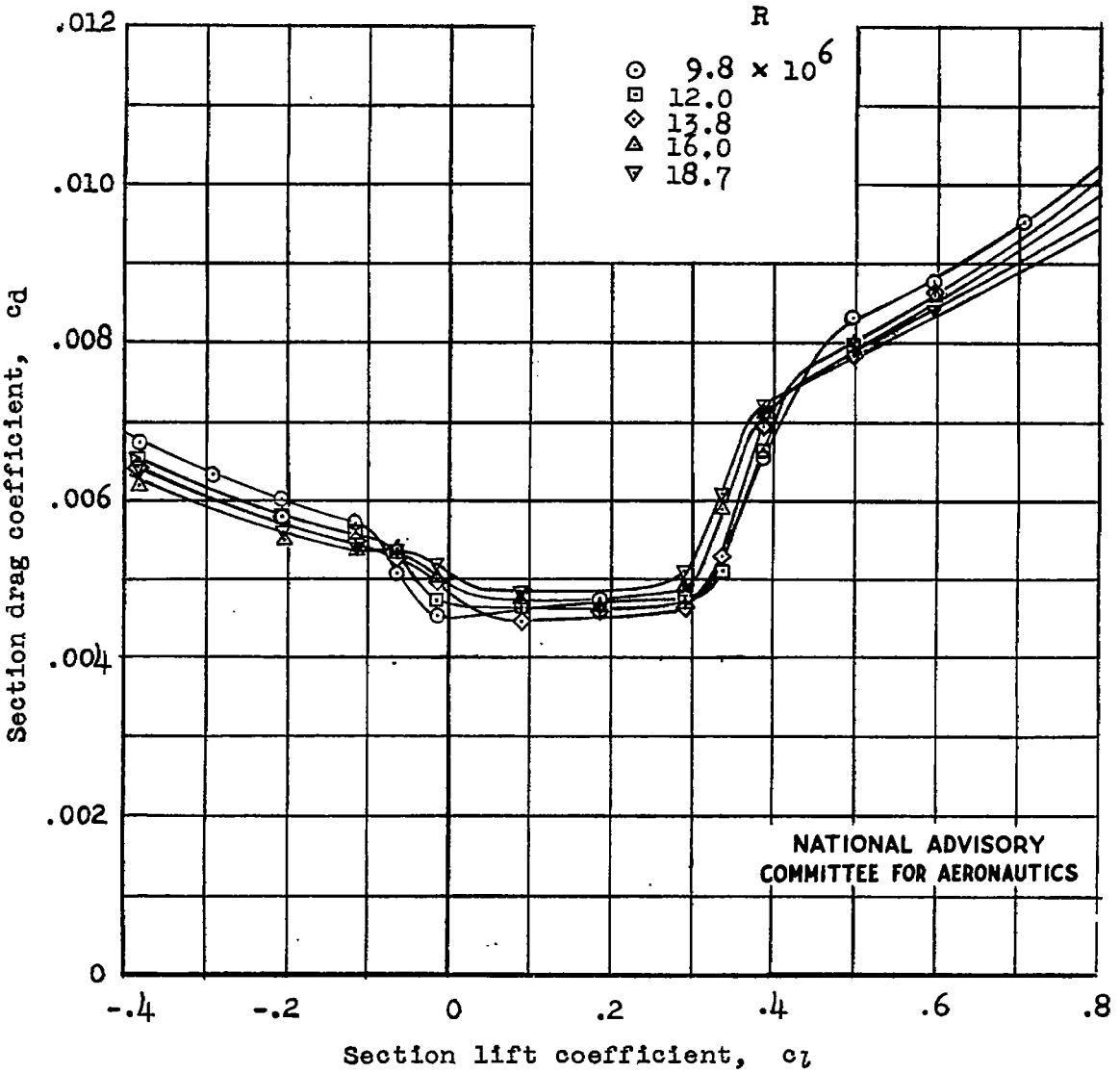


(c) Model with production finish; flap deflected 4°; gap open; test, TDT 958.

Figure 11.- Continued.

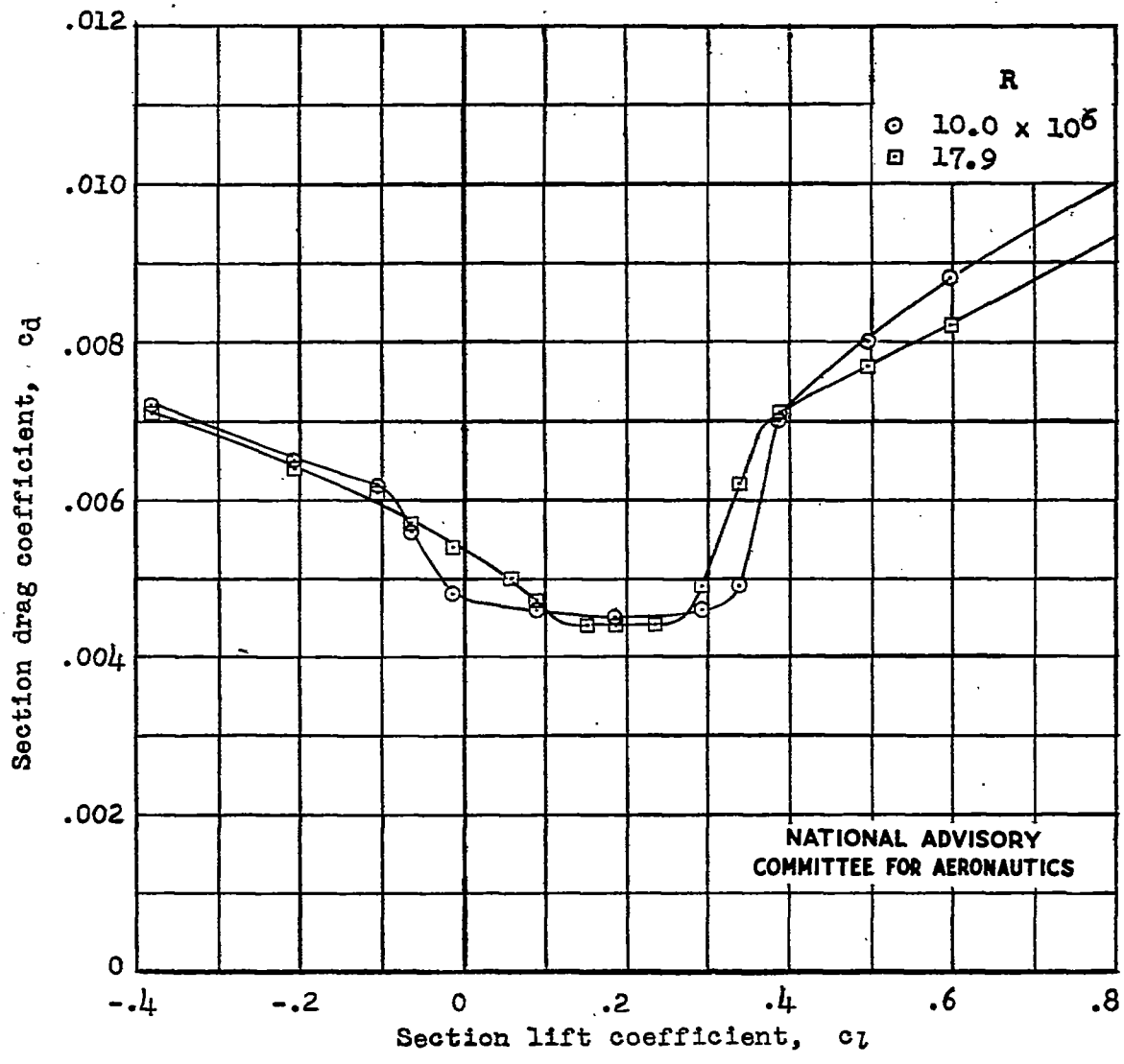


(d) Model with production finish; flap deflected 4°; gap sealed; test, TDT 958.

Figure 11.- Concluded.

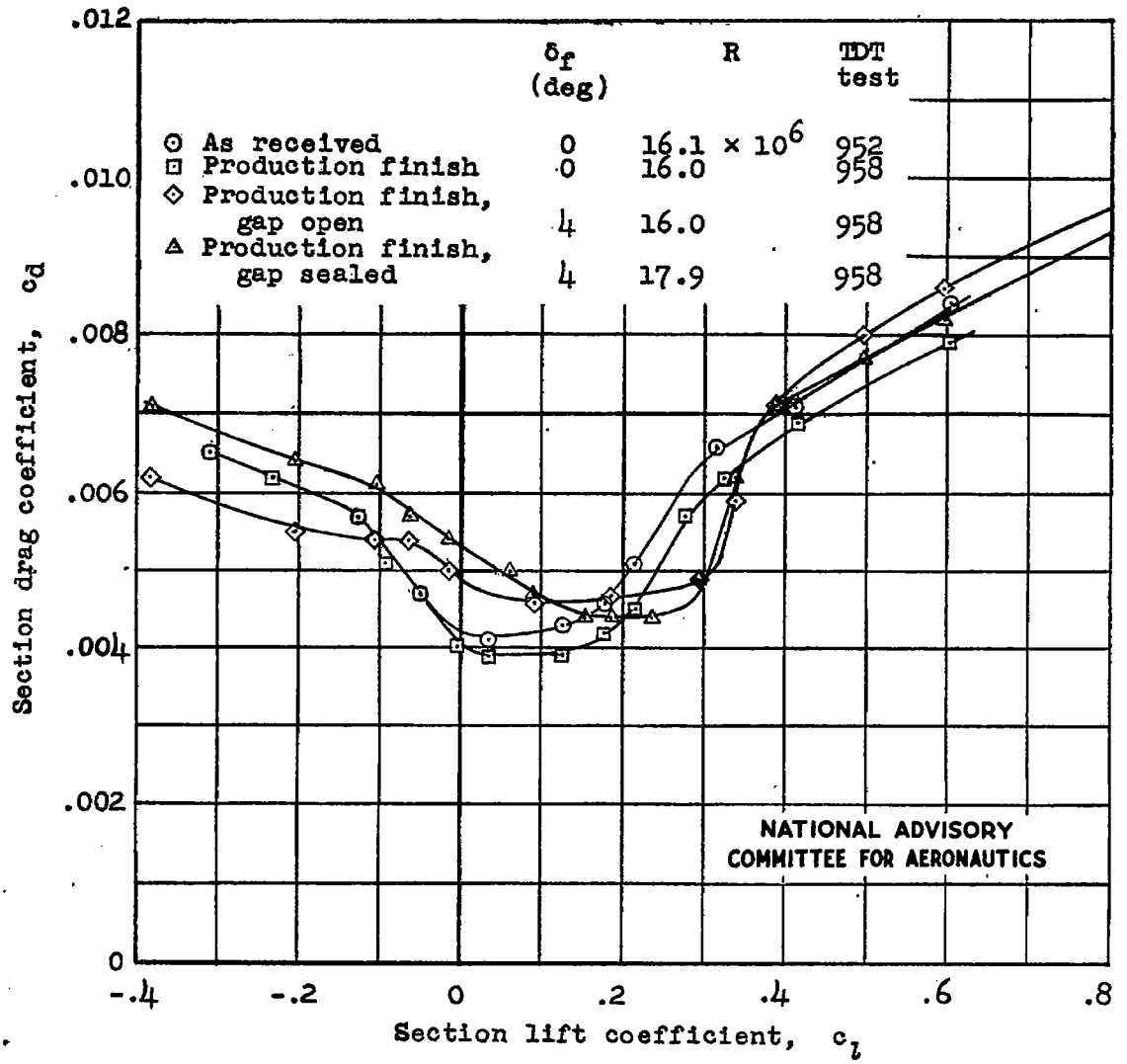


Figure 12.- Effect of changes in surface condition and flap deflection on the variation of section drag coefficient with section lift coefficient for NACA $65_{(215)}$-114 practical-construction airfoil section at approximately constant Reynolds number.